



ISSN 1110-0451



(E S N S A)

## Evaluation of Natural Radioactive Levels and Its Related Potential Radiological Impact of Black Sand in the North of Nile Delta, Egypt

N. M. Hassan<sup>(1)</sup>, B. A. Tartor<sup>(1)</sup>, Nasr Elsayed<sup>(1)</sup> and W. M. Abdellah<sup>(2)\*</sup>

<sup>(1)</sup> Department of Physics, Faculty of Science, Zagazig University, 44519, Zagazig, Egypt

<sup>(2)</sup> Radiation Protection Department, Nuclear and Radiological Safety Research Center, Egyptian Atomic Energy Authority, Cairo, Egypt

### ARTICLE INFO

#### Article history:

Received: 26<sup>th</sup> Mar. 2023

Accepted: 4<sup>th</sup> July 2023

Available online: 12<sup>th</sup> Aug. 2023

#### Keywords:

Radionuclides,

HPGe,

Radiological hazards,

Black Sand,

Egypt.

### ABSTRACT

The objective of this investigation is to quantify the distinct levels of radioactivity exhibited by  $^{238}\text{U}$  ( $^{226}\text{Ra}$ ),  $^{232}\text{Th}$ , and  $^{40}\text{K}$  in samples of black sand that were collected from the northern region of the Nile Delta, in close proximity to Rosetta beach that runs parallel to the Mediterranean shoreline. The specific activities of the radionuclides were measured using a high pure germanium detector (HPGe). The findings indicated that the specific activity levels of  $^{226}\text{Ra}$ ,  $^{232}\text{Th}$ , and  $^{40}\text{K}$  were observed to fall within a range of values from  $10.94 \pm 0.76$  to  $279.31 \pm 16.44$  Bq kg<sup>-1</sup>,  $10.92 \pm 0.67$  to  $665.72 \pm 29.30$  Bq kg<sup>-1</sup>, and  $34.04 \pm 1.68$  to  $101.32 \pm 4.79$  Bq kg<sup>-1</sup>, respectively, with an average value of  $87.85 \pm 5.26$ ,  $155.95 \pm 7.04$ , and  $72.42 \pm 3.65$  Bq kg<sup>-1</sup>, respectively. The concentrations of radionuclides in the samples exceeded the limits recommended by UNSCEAR, the IAEA, and the ICRP for the Earth's crust. Moreover, some samples showed radiological hazard indexes, such as radium equivalent activities ( $\text{Ra}_{\text{eq}}$ ), external and internal indexes, gamma and alpha indexes, and annual effective dose, that exceeded the recommended safety values of 370 Bq kg<sup>-1</sup> for  $\text{Ra}_{\text{eq}}$ , one for external and internal indexes, gamma and alpha indexes, and 0.48 mSv y<sup>-1</sup> for annual effective dose. These findings suggest that black sand samples may pose a radiological hazard, highlighting the need for radiation regulation and regular monitoring of black sand sites.

### INTRODUCTION

The natural radionuclides in the earth's crust, building materials, air, water, food, and the human body, which belong to the  $^{238}\text{U}$ ,  $^{232}\text{Th}$ , and  $^{40}\text{K}$  series, decay over time, leading to the emission of ionizing radiation that humans are exposed to. Soil is considered the primary source of outdoor terrestrial radionuclides due to the presence of these natural radionuclides. However, their distribution is not uniform across soil, sand, and rock, making it vital to comprehend their distribution for the purpose of monitoring and safeguarding against radiation exposure. The external exposures caused by gamma radiation emitted by these radionuclides vary globally [1].

Previous research has shown that after removing light sand with clay, the raw sands were separated using a specific gravity method. In recent years, research on the minerals of heavy sands and concentrates has increased in popularity. The separation of heavy sand minerals into

individual components is a valuable process that relies on specific physical and chemical properties of these minerals, including their particle size, electrical conductivity, and magnetic susceptibility [1, 2].

There are high background radiation areas all over the world. Certain Egyptian regions are known for having high background radiation zones, which have geological and geochemical characteristics that increase natural radiation levels. The Nile Delta near Rosetta beach runs parallel to the Mediterranean coastline is a neighborhood with a high concentration of natural radionuclides, which contributes to an increase in the environmental radiation dose. Black sand contains economic antagonists (ilmenite, zircon, magnetite, rutile, garnet) as well as radioactive materials. Several countries are interested in extracting minerals from black sand for economic purposes, as well as releasing radioactive material that is harmful to the environment [1-3].

Due to the high content in heavy minerals ilmenite, magnetite, garnet, zircon, rutile and black sand monazite, which averages that it is a valuable material for Egyptian income. Several companies are carrying out several projects to make use of the impact of black sand. Therefore, the main purpose of the investigation under consideration is to evaluate the activity concentrations of natural radionuclides  $^{40}\text{K}$ ,  $^{238}\text{U}$  ( $^{226}\text{Ra}$ ) and  $^{232}\text{Th}$  in black sand at the intersection of the North Nile Delta and the Mediterranean Sea coast. The concentrations of radionuclides in black sand samples were compared with global guideline limits. Furthermore, the radium equivalent activity  $\text{Ra}_{\text{eq}}$  and different hazard indices as well as the annual effective dose were calculated and compared to the global safety values recommended by the United Nations Scientific Committee on the Effects of Atomic Radiation's [3].

## MATERIALS AND METHODS

### Sample Preparation

The study involved the collection of twenty-one sediment samples from Rosetta beach, which is situated along the northern coast of the Nile Delta in Egypt, adjacent to the Mediterranean Sea. The survey site was characterized by an open, flat, and almost horizontal terrain. The samples were systematically labeled and their coordinates were recorded using a GPS device (Fig.1). Subsequently, the samples were subjected to homogenization process by passing them through a 1 mm sieve shaker. They were then dried at  $105^\circ\text{C}$  to remove any residual moisture and placed in desiccators for another 24 hours at room temperature. The dried samples were packed in polyethylene containers [100 cm<sup>3</sup>], hermetically sealed with gas tight paraffin, and stored for approximately 30 days to establish equilibrium between  $^{226}\text{Ra}$  and  $^{222}\text{Rn}$  [4]. Throughout the aforementioned time frame, a container with identical geometry to that of the sample was sealed and left untouched for the same period to determine the background radiation. Finally, the specific activity of the samples was measured using gamma spectrometry at the Nuclear and Radiological Safety Research Center in Egypt.

### Measurement of radionuclide concentrations

The specimens were detected within the active region of a shielded High Purity Germanium Detector, the apparatus allowed for the traversal of two concentric cylinders positioned internally, which were constructed from lead, copper, and cadmium materials, along with electronic circuits. A vertical N-type HPGe detector with 40% relative efficiency was utilized to detect 1.33 MeV

photons of  $^{60}\text{Co}$ . This detector was secured by a shield model 747 / 747E, which was composed of an outer shell that was 3/8-inch-thick of steel, an inner layer that was 3/8-inch-thick of steel, and an inner shell that was 3/8-inch-thick of 4-inch bulk shield, the lining is graded with a layer of tin measuring 0.040 inches in thickness, and a layer of copper measuring 0.062 inches in thickness. The spectra were analyzed using the Genie 2000 software [5]. The peak efficiency was determined by employing standard point sources, and the spectrum was analyzed using Genie-2000 Spectroscopy. To achieve energy identification, the calibrated for absolute efficiency using a prepared gamma mixed sources with a various radionuclide in an identical or equivalent shape. The efficiency value was determined by considering the likelihood of decay for each energy, as shown in Equation (1) [6].

$$\varepsilon(E_\gamma) = \frac{\text{NP} \times \text{M}}{t_c \times I_\gamma(E_\gamma) \times A_{\text{Ei}}} \quad (1)$$

In the context of gamma spectroscopy, the detection efficiency at a given energy E is denoted by  $\varepsilon(E_\gamma)$ . NP represents the number of counts below the peak of the considered energy. The concentration of radioactive activity of nuclide I, expressed in Becquerel per kilogram (Bq/kg), can be determined for a peak at energy E using the following formula:

$$A_{\text{Ei}} \left( \frac{\text{Bq}}{\text{kg}} \right) = \frac{\text{NP}}{t_c \times I_\gamma(E_\gamma) \times \varepsilon(E_\gamma) \times \text{M}} \quad (2)$$

The parameters  $t$ ,  $I_\gamma(E_\gamma)$ , and M are essential components in calculating the efficiency of gamma ray detection for a given nuclide. The counting time (t) is measured in seconds and a crucial factor in determining the accuracy of the measurement. The nuclide's probability of gamma emission for a transition at energy  $I_\gamma(E_\gamma)$  is another important factor that contributes to the efficiency of gamma-ray detection. Finally, the mass of the sample (M) is measured in kilograms and is necessary for ensuring quality of the measurement. The IAEA Soil-6 [7] reference material is often used in quality assurance procedures to ensure that measurements are accurate and consistent [7], which has a known concentration of natural radioactivity, was analyzed using gamma spectroscopy. Each sample was counted for 72000 seconds to determine its specific activity, expressed in Bq/kg, of nuclide I. The acquired spectra were analyzed using Genie 2000 program V.3.2 provided by Canberra, which allowed for activity and uncertainty calculation as well as the determination of the Minimum Detectable Activity (MDA) based on Equation 2 [3,8-10].

The current investigation involved measuring the levels of  $^{238}\text{U}$  ( $^{226}\text{Ra}$ ),  $^{232}\text{Th}$ , and  $^{40}\text{K}$  concentrations within the samples over a duration of 72000 seconds. As  $^{226}\text{Ra}$  and its progeny account for the majority (about 98.5%) of the radiological effects of the natural uranium series, the contribution of  $^{238}\text{U}$  and its precursors were disregarded. Consequently,  $^{226}\text{Ra}$  was used as a reference point for the  $^{238}\text{U}$  series, as has been previously established in the literature [11,12]. The specific activity of  $^{226}\text{Ra}$  was determined by analyzing the energies of decay products, namely,  $^{214}\text{Pb}$  at 351.9 keV &  $^{214}\text{Bi}$  at 609.3 keV and 1120 keV. Additionally, the specific activity of thorium  $^{232}\text{Th}$  was estimated by analyzing the gamma rays emitted during the decay of  $^{228}\text{Ac}$  at energies of 911.1 keV and 968.8 keV. Finally, the specific activity of potassium  $^{40}\text{K}$  was estimated by analyzing the gamma ray emitted during the decay of  $^{40}\text{K}$  itself at an energy of 1460.8 keV [8,9], as shown in Fig.2. the potential impact of self-attenuation and coincidence summing was not taken into account [3,8,9].

Each measurement process was accompanied by a calculation of the corresponding statistical error. In order to derive the true activity, present in the sample, we applied appropriate corrections to the observed count rate. These corrections encompass emission probability of emitted radiation, net peak, counter efficiency and mass, and are commonly employed in similar studies. The propagation equation 3 was utilized to compute the error in the Activity. These methods were adopted from references [3,14].

$$\Delta A_{Ei} = A_{Ei} \times \sqrt{\left(\frac{\Delta M}{M}\right)^2 + \left(\frac{\Delta NP}{NP}\right)^2 + \left(\frac{\Delta I_{\gamma}(E_{\gamma})}{I_{\gamma}(E_{\gamma})}\right)^2 + \left(\frac{\Delta t_c}{t_c}\right)^2 + \left(\frac{\Delta \varepsilon(E_{\gamma})}{\varepsilon(E_{\gamma})}\right)^2} \quad (3)$$

**Table (1): Specific activities of  $^{238}\text{U}$ ,  $^{232}\text{Th}$  series and  $^{40}\text{K}$  in black sand samples.**

Sample (ID)	specific activities (Bq kg <sup>-1</sup> )		
	U-238	Th-232	K-40
BS01	159 ± 9.42	290 ± 12.9	62.6 ± 3.08
BS02	170 ± 10.0	305 ± 13.5	65.0 ± 3.19
BS03	195 ± 11.5	366 ± 16.2	66.2 ± 3.27
BS04	213 ± 12.6	406 ± 18.0	67.7 ± 3.27
BS05	23.7 ± 1.76	24.2 ± 1.60	62.7 ± 4.10
BS06	10.9 ± 0.76	10.9 ± 0.67	97.6 ± 4.59
BS07	140 ± 8.27	218 ± 9.66	56.1 ± 2.78
BS08	59.3 ± 3.71	87.9 ± 4.06	70.5 ± 3.95
BS09	42.1 ± 2.52	62.4 ± 2.82	34.0 ± 1.68
BS10	61.1 ± 3.69	80.3 ± 3.68	68.6 ± 3.30
BS11	109.0 ± 6.47	164 ± 7.31	53.5 ± 2.68
BS12	22.4 ± 1.42	26.1 ± 1.32	78.4 ± 3.73
BS13	58.4 ± 3.51	75.7 ± 3.46	61.8 ± 3.03
BS14	13.2 ± 0.88	10.6 ± 0.58	76.3 ± 3.64
BS15	54.0 ± 2.77	60.7 ± 3.07	75.0 ± 4.20
BS16	12.71 ± 0.86	15.2 ± 0.84	76.9 ± 3.70
BS17	14.03 ± 0.97	15.2 ± 0.88	83.7 ± 4.07
BS18	10.94 ± 0.76	10.9 ± 0.67	97.6 ± 4.59
BS19	20.96 ± 1.37	30.57 ± 1.55	101 ± 4.79
BS20	176 ± 10.7	349 ± 15.8	76.2 ± 4.82
BS21	279 ± 16.4	666 ± 29.3	89.1 ± 4.19
<b>Average</b>	<b>87.9 ± 5.26</b>	<b>156 ± 7.04</b>	<b>72.4 ± 3.65</b>

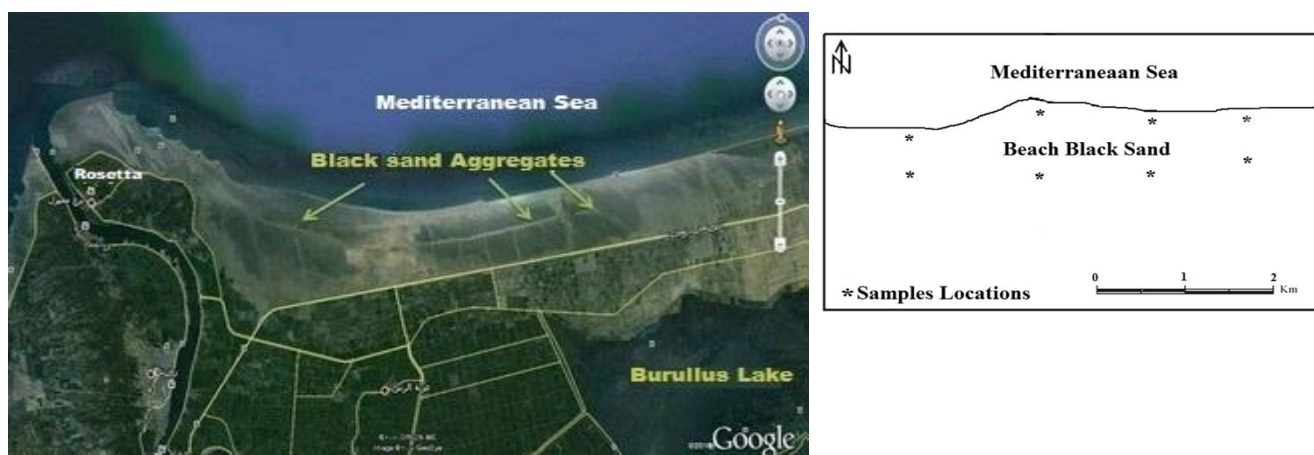


**Fig. (1): The map of the locations of the collected black sand samples.**

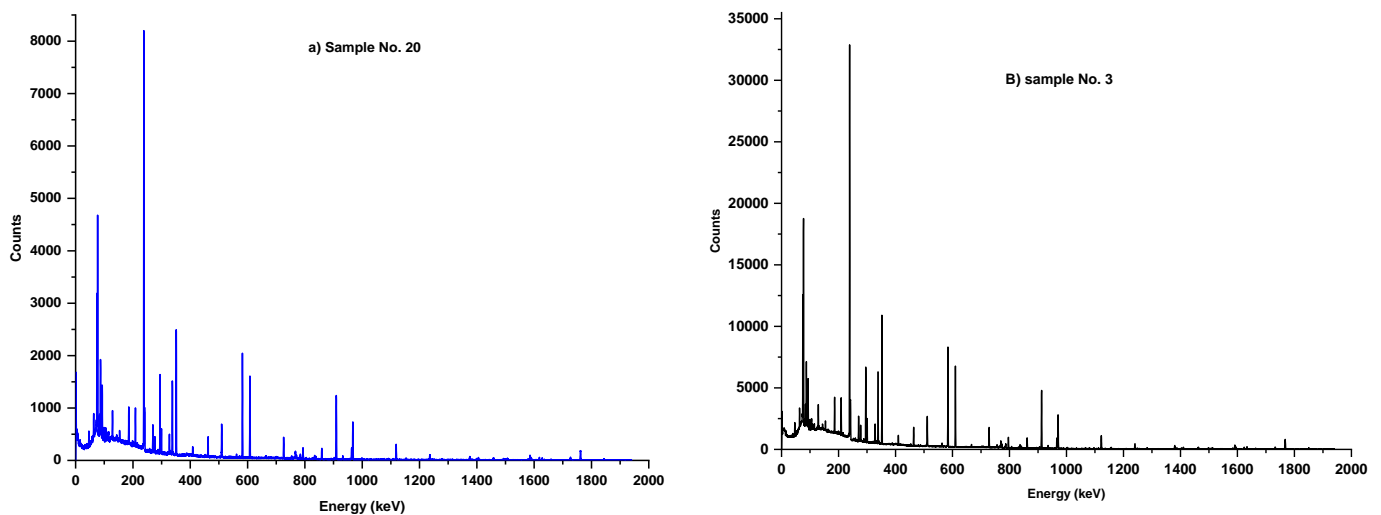


Fig. (2): The typical gamma ray spectrum of radionuclide of  $^{226}\text{Ra}$ ,  $^{232}\text{Th}$  and  $^{40}\text{K}$  of black sand samples, [20(a) & 3(b)].

## RESULTS AND DISCUSSIONS

The findings of the current study have been exhibited in Table 1. The specific activities of  $^{226}\text{Ra}$ ,  $^{232}\text{Th}$  and  $^{40}\text{K}$  in the materials that were analyzed ranged from  $10.9 \pm 0.76$  (BS06) to  $279 \pm 16.4$  (BS21)  $\text{Bq kg}^{-1}$ , with an average value of  $87.9 \pm 5.26$   $\text{Bq kg}^{-1}$  for  $^{226}\text{Ra}$ ,  $10.6 \pm 0.58$  (BS14) to  $666 \pm 29.3$  (BS21)  $\text{Bq kg}^{-1}$ , with an average value of  $156 \pm 7.04$   $\text{Bq kg}^{-1}$  for  $^{232}\text{Th}$ , and from  $34.0 \pm 1.68$  (BS09) to  $101 \pm 4.79$  (BS19)  $\text{Bq kg}^{-1}$ , with an average value of  $72.4 \pm 3.65$   $\text{Bq kg}^{-1}$  for  $^{40}\text{K}$ . These values have been tabulated in Table 1 and illustrated in Fig. 3. It has been observed from Fig. 3 that the  $^{232}\text{Th}$  content in all samples is higher compared to other radionuclides such as  $^{226}\text{Ra}$  and  $^{40}\text{K}$ . The maximum levels of the measured radionuclides in selected samples were  $279.31 \pm 16.44$  (BS21)  $\text{Bq kg}^{-1}$  for  $^{226}\text{Ra}$ ,  $665.72 \pm 29.30$  (BS21)  $\text{Bq kg}^{-1}$  for  $^{232}\text{Th}$ , and  $101.32 \pm 4.79$  (BS19)  $\text{Bq kg}^{-1}$  for  $^{40}\text{K}$ . The results of this study suggest that the specific activity in the selected samples in Egypt is relatively higher than the global average specific activity concentrations in the earth crust, which are 35, 30, and 400  $\text{Bq kg}^{-1}$  for Ra-226, Th-232, and K-40, respectively, as reported in UNSCEAR[3,19]. The values of natural radionuclides in other previous studies in Egypt and other countries have been summarized in Table 2. This variation in the radionuclide concentrations may be attributed to weathering processes, which increase the radionuclide content of black sand[2].

The radium equivalent activity ( $Ra_{eq}$ ) has been developed by UNSCEAR with the purpose of computing the radiation risks associated with the materials

maintained at different levels of  $^{226}\text{Ra}$ ,  $^{232}\text{Th}$ , and  $^{40}\text{K}$  in a single quantity [3, 9, 19], Eq. 4.

$$Ra_{eq} = C_{Ra} + 1.43C_{Th} + 0.077C_K \quad (4)$$

The concentrations of  $^{226}\text{Ra}$ ,  $^{232}\text{Th}$ , and  $^{40}\text{K}$  in  $\text{Bq kg}^{-1}$  are represented by  $A_{Ra}$ ,  $A_{Th}$ , and  $A_K$ , respectively. The radium equivalent index was derived with the presumption that the equivalent dose of gamma ray produced by 370  $\text{Bq kg}^{-1}$  of  $^{226}\text{Ra}$ , 259  $\text{Bq kg}^{-1}$  of  $^{232}\text{Th}$ , and 4810  $\text{Bq kg}^{-1}$  of  $^{40}\text{K}$  is the same. To maintain the gamma ray dose below  $1.5 \text{ mS y}^{-1}$ , the material's  $Ra_{eq}$  activity concentration ought to be lower than 370  $\text{Bq kg}^{-1}$  [21]. Radium equivalent concentration in samples was ranged from  $34.1 \pm 2.07$   $\text{Bq kg}^{-1}$  (BS06) to  $1238 \pm 58.66$   $\text{Bq kg}^{-1}$  (BS21) with a average value  $316.4 \pm 15.6$   $\text{Bq kg}^{-1}$ , as illustrated in Table 3. In this investigation, certain Black sand samples were found to have a Radium equivalent value that went beyond the suggested threshold of 370  $\text{Bq kg}^{-1}$ , indicating a potential radiological hazard associated with these materials.

### External and internal hazard indices ( $H_{ex}$ , $H_{in}$ )

The selected samples were analyzed to calculate their external and internal hazard indices as illustrated in Eqs.(5 &6). [9, 22]

$$H_{ex} = \frac{C_{Ra}}{370} + \frac{C_{Th}}{259} + \frac{C_K}{4810} \leq 1 \quad (5)$$

$$H_{in} = \frac{C_{Ra}}{185} + \frac{C_{Th}}{259} + \frac{C_K}{4810} \leq 1 \quad (6)$$

The amounts of  $^{226}\text{Ra}$ ,  $^{232}\text{Th}$ , and  $^{40}\text{K}$  are expressed as  $C_{Ra}$ ,  $C_{Th}$ , and  $C_K$  in  $\text{Bq/kg}$ . The UNSCEAR safety guidelines state that a material's external and internal hazard

indices must be lower than unity in order to keep the external gamma radiation dosage to less than 1.5 mSv y<sup>-1</sup> [18]. In this investigation, the external danger index was found to have an average value of 0.85 0.04 (as presented in Tables 3). A few samples exhibited external hazard indices that surpassed the recommended limit, suggesting that there may be external radiation hazards associated with these samples. Furthermore, the average of the internal hazard

index for all samples was determined to be  $1.09 \pm 0.06$  (as shown in Table 3), which exceeds the recommended threshold. Thus, the use of black sand may pose potential radiation risks as these materials typically retain natural radionuclides, which can serve as a source of radiation exposure for residents and workers. Therefore, regular monitoring of radiation exposure is highly recommended for the sake of public and environmental safety.

**Table (2): The concentrations of <sup>238</sup>U (<sup>226</sup>Ra), <sup>232</sup>Th series and <sup>40</sup>K in this study as well as the studies for various countries.**

	Country	Sample Type	Activity concentrations (Bq kg <sup>-1</sup> )			Ref.
			U-238 Average	Th-232 Average	K-40 Average	
-	<b>Egypt</b>	Black Sand	87.85±5.26	155.95±7.04	72.42±3.65	Present Study
1	<b>Egypt - North of Nile Delta near Rosetta beach</b>	Black Sand	107.6±40.2	201.6±84.8	116.2±25.2	[1]
2	<b>Egypt - Tamsah Lake beach in Suez Canal region</b>	Black Sand sediment samples	10.86±2.17 8.64±2.49	11.41±3.28 13.77±4.61	327.65±80.05 141.64±43.01	[26]
3	<b>Egypt - North east of Nile Delta</b>	Black Sand - soil samples	21.4±0.74	26.3± 0.88	270.7±4.64	[27]
4	<b>Egypt - Baltim Area</b>	Black Sand - shore sediment samples	38.2±1.20	54.3±1.38	265.6±4.43	
		Black Sand Dunes - used in the manufacturing of building bricks	32.11	24.36	147.4	[28]
5	<b>Egypt - Western Coast of Suez Gulf</b>	Soil and Beach Samples	9.9±0.8	6.6±0.9	172.15±5.4	[29]
6	<b>Egypt - Red sea (safaga)</b>	sand dunes	28.82	14.03	558.39	[30]
7	<b>Egypt - East Rosetta Estuary</b>	beach sands	778.2	1510.25	8.41	[31]
8	<b>Egypt - Mediterranean and Red Seas (Resort sites)</b>	beach sand	39±15	21±13	402±23	[32]
9	<b>India - Rameshwaram Island, Tamilnadu</b>	Coastal Sediments	9.59	17.64	298.47	[33]
10	<b>India - Kerala, Chavara-Neendakara (High Background Radiation Area along the Southwest coast of India (Kerala))</b>	Placer Deposits	2310	12668	1670.4	[34]
11	<b>India - North East Coast of Tamilnadu</b>	Beach Sediments	8.39±4.87	24.52±4.73	274.87±25.58	[35]
12	<b>Sri Lanka - the West Coast</b>	beach sand	268±6.8	1032±20	327±34.8	[36]
13	<b>Turkey - Black Sea coast of Kocaeli</b>	beach sand samples	4.417 - 14.047	2.627 - 16.557	11.607-513	[37]
14	<b>Turkey - Aegean Sea (in Didim and Izmir Bay)</b>	sediment samples	9±0.6 - 12±0.7	6±0.3 - 16±1.0	250±13 - 665±33	[38]
15	<b>Oman - along the northern coast of Oman Sea</b>	marine sediments	11.83 - 22.68	10.70 -25.02	222.89 - 535.07	[39]

**Radium equivalent concentration (Ra<sub>eq</sub>);**

**Table (3): Radium equivalent, external and internal hazard indices of Black sand samples.**

Sample Code	Radium equivalent ( $R_{eq}$ ) ( $Bq\ Kg^{-1}$ )	Internal index ( $H_{in}$ )	External index ( $H_{ex}$ )
BS01	579 ± 28.1	2.00 ± 0.10	1.56 ± 0.08
BS02	611 ± 29.6	2.11 ± 0.11	1.65 ± 0.08
BS03	723 ± 34.9	2.48 ± 0.13	1.95 ± 0.09
BS04	800 ± 38.4	2.74 ± 0.14	2.16 ± 0.10
BS05	63.1 ± 4.37	0.24 ± 0.02	0.17 ± 0.01
BS06	34.1 ± 2.07	0.12 ± 0.01	0.09 ± 0.01
BS07	456 ± 22.3	1.61 ± 0.08	1.23 ± 0.06
BS08	191 ± 9.82	0.67 ± 0.04	0.51 ± 0.03
BS09	134 ± 6.68	0.48 ± 0.03	0.36 ± 0.02
BS10	181 ± 9.20	0.66 ± 0.04	0.49 ± 0.03
BS11	348 ± 17.1	1.23 ± 0.06	0.94 ± 0.05
BS12	65.8 ± 3.59	0.24 ± 0.01	0.18 ± 0.01
BS13	172 ± 8.69	0.62 ± 0.03	0.46 ± 0.02
BS14	34.3 ± 1.99	0.13 ± 0.01	0.09 ± 0.01
BS15	147 ± 7.49	0.54 ± 0.03	0.40 ± 0.02
BS16	40.3 ± 2.35	0.14 ± 0.01	0.11 ± 0.01
BS17	42.1 ± 2.55	0.15 ± 0.01	0.11 ± 0.01
BS18	34.1 ± 2.07	0.12 ± 0.01	0.09 ± 0.01
BS19	72.5 ± 3.95	0.25 ± 0.01	0.20 ± 0.01
BS20	681 ± 33.7	2.32 ± 0.12	1.84 ± 0.09
BS21	1238 ± 58.66	4.10 ± 0.20	3.34 ± 0.16
<b>Average</b>	<b>316.44 ± 15.60</b>	<b>1.09 ± 0.06</b>	<b>0.85 ± 0.04</b>

**Table (4) Absorbed dose rate, annual effective dose, gamma and alpha Indices of black sand samples.**

Sample Code	The absorbed dose rate ( $D$ , $nGy\ h^{-1}$ )	The annual effective dose ( $E$ , $mSv\ y^{-1}$ )	Gamma Index: radioactivity level index ( $I_\gamma$ )	Alpha Index $I_\alpha$
BS01	256 ± 12.5	0.315 ± 0.015	2.00 ± 0.097	0.796 ± 0.047
BS02	271 ± 13.2	0.332 ± 0.016	2.114 ± 0.102	0.848 ± 0.050
BS03	320 ± 15.5	0.393 ± 0.019	2.501 ± 0.120	0.974 ± 0.058
BS04	354 ± 17.1	0.434 ± 0.021	2.765 ± 0.133	1.067 ± 0.063
BS05	28.6 ± 1.98	0.035 ± 0.002	0.221 ± 0.015	0.119 ± 0.009
BS06	15.9 ± 0.96	0.020 ± 0.001	0.124 ± 0.007	0.055 ± 0.004
BS07	202 ± 9.94	0.248 ± 0.012	1.574 ± 0.077	0.698 ± 0.041
BS08	84.9 ± 4.40	0.104 ± 0.005	0.660 ± 0.034	0.296 ± 0.019
BS09	59.6 ± 2.99	0.073 ± 0.004	0.464 ± 0.023	0.211 ± 0.013
BS10	81.0 ± 4.13	0.099 ± 0.005	0.628 ± 0.032	0.306 ± 0.018
BS11	154 ± 7.64	0.190 ± 0.009	1.201 ± 0.059	0.545 ± 0.032
BS12	29.9 ± 1.63	0.037 ± 0.002	0.231 ± 0.013	0.112 ± 0.007
BS13	76.6 ± 3.90	0.094 ± 0.005	0.594 ± 0.030	0.292 ± 0.016
BS14	15.9 ± 0.92	0.020 ± 0.001	0.123 ± 0.007	0.066 ± 0.004
BS15	65.8 ± 3.37	0.081 ± 0.004	0.508 ± 0.026	0.270 ± 0.014
BS16	18.5 ± 1.07	0.023 ± 0.001	0.144 ± 0.008	0.064 ± 0.004
BS17	19.4 ± 1.17	0.024 ± 0.001	0.150 ± 0.009	0.070 ± 0.005
BS18	15.9 ± 0.96	0.020 ± 0.001	0.124 ± 0.007	0.055 ± 0.004
BS19	32.9 ± 1.80	0.040 ± 0.002	0.256 ± 0.014	0.105 ± 0.007
BS20	301 ± 15.0	0.370 ± 0.018	2.357 ± 0.116	0.881 ± 0.054
BS21	546 ± 26.0	0.673 ± 0.0319	4.289 ± 0.203	1.397 ± 0.082
<b>Average</b>	<b>141 ± 6.95</b>	<b>0.17 ± 0.01</b>	<b>1.10 ± 0.05</b>	<b>0.44 ± 0.03</b>

### The absorbed dose rate in air

The absorbed dose rate in air (ADRA) is a parameter used to quantify the amount of gamma radiation absorbed by the atmosphere at a height of 1 meter above ground level. To determine ADRA, the concentrations of radioisotopes  $^{226}\text{Ra}$ ,  $^{232}\text{Th}$ , and  $^{40}\text{K}$  present in the surrounding environment are taken into account. The calculation of ADRA is carried out using Equation 7, which includes the corresponding concentrations of the three aforementioned radioisotopes,  $C_{\text{Ra}}$ ,  $C_{\text{Th}}$  and  $C_{\text{K}}$ . This method is commonly used in scientific studies and publications [15,16].

$$ADRA \left( \frac{\text{nGy}}{\text{h}} \right) = (0.462C_{\text{Ra}}) + (0.661C_{\text{Th}}) + (0.042C_{\text{K}}) \quad (7)$$

In order to determine the effective dose received by adults from the absorbed dose rate in air, a conversion coefficient of 0.7 Sv/Gy is typically employed. The calculation also takes into account the occupancy factor of 0.2 [3, 18]. By incorporating these parameters into the calculation, the absorbed dose rate in air can be transformed into the effective dose received by adults. This conversion method is commonly used in scientific research and publications.

The results of the calculation show that the absorbed dose rate in air for the samples varied from  $15.9 \pm 0.92$  nGy h<sup>-1</sup> (BS14) to  $546 \pm 26.0$  nGy h<sup>-1</sup> (BS21), with an average value of  $141 \pm 6.95$  nGy h<sup>-1</sup>. These values indicate the level of radiation exposure in the samples. It is important to note that exposure to high levels of radiation can have detrimental effects on human health,

including an increased risk of cancer and other illnesses. Therefore, it is crucial to monitor radiation levels in the environment and take appropriate precautions to minimize exposure. Many of the selected samples had absorbed radiation dose values that exceeded the UNSCEAR recommended values.[3], i.e., 59 nGy h<sup>-1</sup> as illustrated in Table 4. As a result, those samples are at risk of radiation exposure. Therefore, black sand samples should be used under regulation precautions, especially if used as dwelling building materials.

### Annual effective dose;

The authors of this study employed Equation (8)[8, 9, 19] to calculate the annual effective dose (AED) resulting from the emission of gamma rays by  $^{226}\text{Ra}$ ,  $^{232}\text{Th}$ , and  $^{40}\text{K}$  in the analyzed samples. This method is frequently utilized in scientific research and publications.

$$AED_{out} \left( \frac{\text{mSv}}{\text{y}} \right) = ADRA \left( \frac{\text{nGy}}{\text{h}} \right) \times 8760 \left( \frac{\text{h}}{\text{y}} \right) \times 0.2 \times 0.7 \left( \frac{\text{Sv}}{\text{Gy}} \right) \quad (8)$$

The authors employed the equation 8 for their calculations. The computed AED of gamma rays varied between  $0.020 \pm 0.001$  mSv y<sup>-1</sup> (BS14) and  $0.670 \pm 0.0319$  mSv y<sup>-1</sup> (BS21) with an average value of  $0.17 \pm 0.01$  mSv y<sup>-1</sup>, as introduced in Table 4 and figure 4. Notably, the AED values were found to be lower than the global average AED of 0.48 mSvy<sup>-1</sup> (480 μSvy<sup>-1</sup>) [19]. Additionally, the computed AED values were much lower than the recommended AED values of 1 mSv for the general public and 20 mSv for occupational, as stipulated by the International Commission on Radiation Protection, [ICRP-103][21].

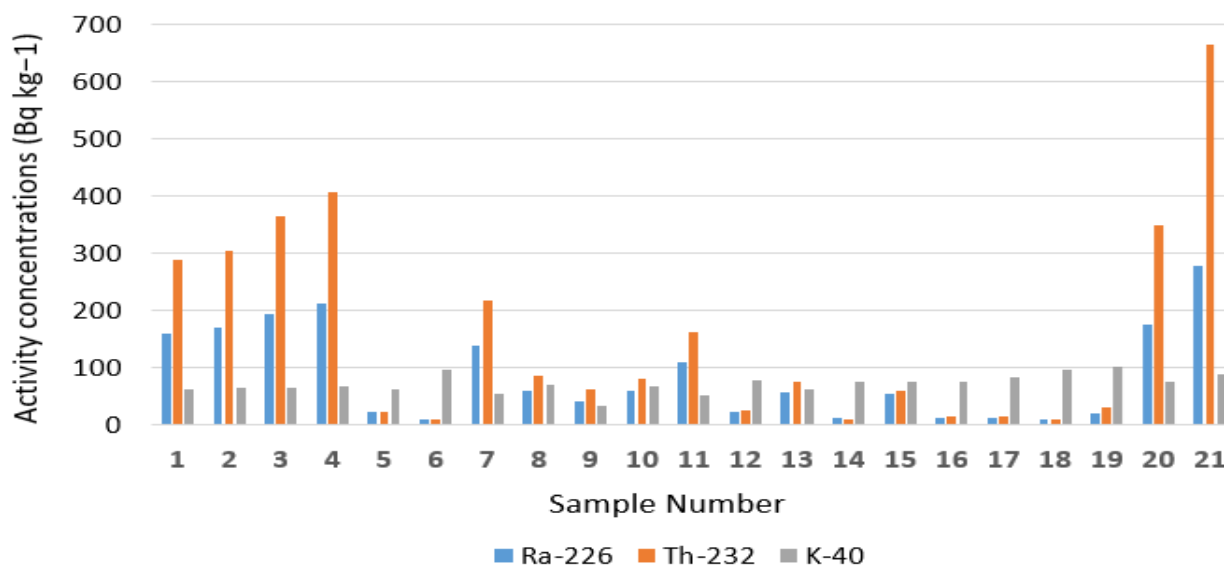
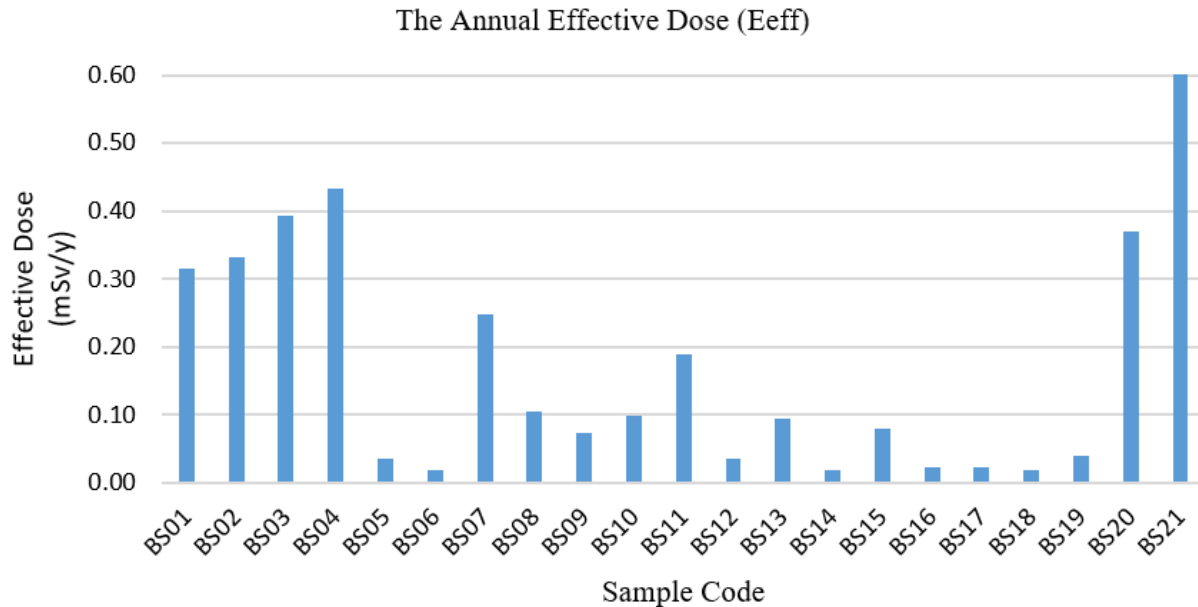


Fig. (3): The specific activities of  $^{238}\text{U}$  ( $^{226}\text{Ra}$ ),  $^{232}\text{Th}$  series and  $^{40}\text{K}$  of the studied samples.



**Fig. (4): The annual effective gamma dose of back sand samples.**

#### The gamma and Alpha radiation hazards indices;

The potential risks of gamma ray radiation resulting from natural radionuclides in materials can be evaluated through the use of the gamma index, ( $I_\gamma$ ) which represents the average of the radioactivity level index. As per the guidelines established by the European Commission,  $I_\gamma$  should be less than 1 to ensure that the gamma radiation dose does not exceed 1 mSv  $y^{-1}$  [23, 24]. Equation 9 can be employed to determine the gamma ray index ( $I_\gamma$ ).

$$I_\gamma = \frac{C_{Ra}}{300} + \frac{C_{Th}}{200} + \frac{C_K}{3000} \quad (9)$$

The  $I_\gamma$  of the samples varied from  $0.123 \pm 0.007$  for (BS14) to  $4.29 \pm 0.20$  for (BS21) with a average value of  $1.10 \pm 0.05$ , as seen in Table 4. Several samples had a radioactivity level  $<1$  so that these samples haven't pose radiation risk and can be safely handled without special precautions, whereas a few samples had a radioactivity level  $>1$  so that these samples pose radiation risk and should be handled under radiation regulation precautions [8].

The alpha radiation resulting from the release of radon from samples is commonly referred to as the alpha index ( $I_\alpha$ ). This index can be computed using Equation 10 [8, 9]. To keep the radium concentration below the recommended upper limit of 200 Bq  $kg^{-1}$ , continual efforts are required to monitor and control radium levels., the alpha index should be less than or equal to 1, resulting in a maximum released radon concentration of less than 200 Bq  $m^{-3}$ . The alpha index can be determined using the following formula.

$$I_\alpha = \frac{C_{Ra}}{200} \quad (10)$$

The Alpha index of the samples varied from  $0.055 \pm 0.004$  (BS18) to  $1.397 \pm 0.082$  (BS21) with a average value of  $0.439 \pm 0.026$ , as seen in Table 4. The study found that the Alpha index values for most of the samples were lower than unity, indicating that they pose no radiation hazards for workers and the public. However, two samples (BS04 and BS21) had values higher than unity, suggesting that they contain radium concentrations greater than 200 Bq  $kg^{-1}$ , which could lead to indoor radon levels exceeding 200 Bq  $m^{-3}$ . Therefore, it is recommended to measure the radon exhalation rates to ensure worker safety. It should be noted that the radium concentration, as well as the texture and size of grains and the permeability of materials, have significant effects on the radon exhalation rate, as explained in the study by Hassan et al., 2010 [12].

#### CONCLUSIONS

The study investigated the concentrations of natural radionuclides in black sand samples collected from the Rosetta beach in Egypt, specifically  $^{226}Ra$ ,  $^{232}Th$ , and  $^{40}K$ . The results indicated that the concentration levels for each of these radionuclides ranged from  $10.9 \pm 0.76$  (BS06) to  $279 \pm 16.4$  (BS21) Bq  $kg^{-1}$ ,  $10.6 \pm 0.58$  (BS14) to  $666 \pm 29.3$  (BS21) Bq  $kg^{-1}$ , and  $34.0 \pm 1.68$  (BS09) to  $101 \pm 4.79$  (BS19) Bq  $kg^{-1}$  respectively. The concentration levels were discovered to exceed the limits recommended by UNSCEAR[21] and ICRP [19] for radionuclides levels present in the Earth's crust.

The study also evaluated the radiological hazard indexes for the black sand samples, including radium equivalent activities [ $Ra_{eq}$ ], external and internal indexes, gamma and alpha indexes. The findings indicated that some of the samples had radiological hazard indexes that exceeded the recommended values of 370 Bqkg<sup>-1</sup>, 1, and 1, respectively.

Despite the high concentration levels and radiological hazard indexes observed in some samples, the research discovered that the yearly effective dose remained lower than the global average yearly efficient dosage of 0.48 mSvy<sup>-1</sup>, and significantly lower than the recommended values of 1 mSv for the public or 20 mSv for occupational dose set by ICPR and IAEA[24].

## REFERENCES

- [1] Fawzia Mubarak, M. Fayez-Hassan, N. A. Mansour, Talaat Salah Ahmed & Abdallah Ali. (2017). Radiological Investigation of High Background Radiation Areas. Scientific REPOrTS | 7: 15223 | DOI:10.1038/s41598-017-15201-2
- [2] Abdallah, W. M. (2019). sequential Radiochemical Procedure for Isotopic Analysis of Uranium and Thorium in Egyptian Monazite. Radiochemistry, Vol. 61, No. 4, pp. 470–477
- [3] United Nations Scientific Committee on the Effects of Atomic Radiation. (2000). Sources and Effects of Ionizing Radiation, Report to the General Assembly. United Nations.
- [4] Pimpl M, Yoo B, Yordanova I. (1992). Optimization of a radioanalytical procedure for the determination of uranium isotopes in environmental samples. J Radioanal Nucl Chem; 161:437–441
- [5] Canberra Industries, USA, Genie™ 2000 Spectroscopy Software, Operations V3.1 in 1 Apr 2003.
- [6] Abdallah W. M., Diab H. M., El-Kameesy S. U., Salama E. & El-Framawy S., (2017). Natural radioactivity levels and associated health hazards from the terrestrial ecosystem in Rosetta branch of the River Nile, Egypt. ISOTOPES IN ENVIRONMENTAL AND HEALTH STUDIES, <http://dx.doi.org/10.1080/10256016.2017.1293668>
- [7] Pszonicki, L., A.N. Hanna, A.N., and Suschny, O., (1984). Report on Intercomparison IAEA/SOIL-6, International Atomic Energy Agency, IAEA/RL/111.
- [8] N. M. Hassan & J. S. Chae. (2019). Radioactivity and radiological impact of industrial raw materials in Korea. International Journal of Environmental Science and Technology, pp. 1–8
- [9] N. M. HASSAN ET AL. (2019). Assessment of Radiological Hazards of Using Petroleum Raw Materials And Their WASTE. Radiation Protection Dosimetry, pp. 1–13
- [10] Torres Astorga, R., Rizzotto, M.G., Velasco, H. (2019). Improving the efficiency in the detection of gamma activities in environmental soil samples: influence of the granulometry and soil density. Journal of Radioanalytical and Nuclear Chemistry Vol. 321:805–814.
- [11] Hassan, N. M., Mansour, N. A., Fayez-Hassan, M. and Fares, S. (2017). Assessment of radiation hazards due to exposure to radionuclides in marble and ceramic commonly used as decorative building material in Egypt. Indoor Built Environ. 26(3), 317–326.
- [12] Hassan, N. M., Mansour, N. A., Fayez-Hassan, M. and Sedqy, E. (2016). Assessment of natural radioactivity in fertilizers and phosphate ores in Egypt. J. Taibah Univ. Med. Sci. 10, 296–306.
- [13] Lépy, M C., Pearce, A., and Sima, O., (2015). Uncertainties in gamma-ray spectrometry. journal of Metrologia 52, S123–S145.
- [14] Guembou, S. C. J., Samafou, P., Moyo M. N., Gregoire, C., Eric J. N. M., Alexandre, N. E., Motapon, O., and Strivay, D. (2017). Precision measurement of radioactivity in gamma-rays spectrometry using two HPGe detectors comparison techniques: Application to the soil measurement. journal of MethodsX V.4, 42–54.
- [15] Beck, H.L. (1980). Exposure Rate Conversion Factors for Radionuclides Deposited on the Ground. Report no.EML-378.NY. US, Department of Energy.
- [16] International Commission on Radiological Protection (1991): Recommendations of the International Commission on Radiological Protection, Annals of the ICRP, 21, 1-3.-473.
- [17] UNSCEAR. United Nations Scientific Committee on the Effects of Atomic Radiation. (1993). New York: Sources and effects of ionizing radiation
- [18] UNSCEAR (1988). United Nations Scientific Committee on the Effects of Atomic Radiation. Sources and Biological Effects of Ionizing Radiation, United Nations, New York.
- [19] United Nations Scientific Committee on the Effects of Atomic Radiation. (2008). Sources and Effects of Ionizing Radiation, Report to the General Assembly. United Nations.
- [20] Chiozzi, P., Pasquale, V., Verdoya, M. (2002): Naturally occurring radioactivity at the Alps-Appennines transition. Radiat. Meas. 35, 147-154.
- [21] ICRP, International Commission on Radiological Protection. (2007). The 2007 Recommendation of the

- International Commission on Radiological Protection (Oxford: ICRP; ICRP Publication)103
- [22] Beretka, J., Matthew, P.J. (1985). Natural radioactivity of Australian building materials, industrial wastes and by-products. *Health Phys.* 48, 87.
- [23] International Atomic Energy Agency. (1994), International basic safety standards for the protection against ionizing radiation and for the safety of radiation sources. GOV/2715/Vienna.
- [24] International Atomic Energy Agency. (2014). Radiation protection and safety of radiation sources: international basic safety, standards. Part 3 No. GSR Part 3. IAEA, Vienna, Austria.
- [25] Hassan NM, Ishikawa T, Hosoda M, Sorimachi A, Tokonami S, Fukushi M, Sahoo SK. (2010). Assessment of the natural radioactivity using two techniques for the measurement of radionuclide concentration in building materials used in Japan. *J Radioanal Nucl Chem* 283:15–21
- [26] S. Fares. (2017). Measurements of natural radioactivity level in black sand and sediment samples of the Tamsah Lake beach in Suez Canal region in Egypt. *Journal of Radiation Research and Applied Sciences* 10 (2017) 194-203
- [27] W.A. Mowafi and M.S. El-Tahawy. (2009). RADIOLOGICAL INVESTIGATION OF THE BLACK SAND REGION OF THE NORTH-EAST OF THE NILE DELTA. Proceedings of the 7th Conference on Nuclear and Particle Physics, 11-15 Nov. 2009, Sharm El-Sheikh, Egypt (P 503-508)
- [28] Abdel-Razek, Y. A., El-Kassas, H. I, Al-Mobaid, A. M, Bakhit A. A. (2016). Test of the Null Hypothesis on the Radiation Hazards of the Random Public Uses of the Black Sand Dunes at Baltim Area. *International Journal of Research Studies in Biosciences (IJRSB)*. Volume 4, Issue 5, May 2016, PP 50-56
- [29] E. Salama, H.M. Diab, S.A. EL-Fiki, A. Ibrahim. (2015). Distribution of Radionuclides in Soil and Beach Samples of the Western Coast of Suez Gulf, Egypt. *Arab Journal of Nuclear Science and Applications*, 48(2), (63-69)
- [30] A. El-Taher, H.A. Madkour. (2013). Texture and environmental radioactivity measurements of Safaga sand dunes. *Indian Journal of Geo-Marine Sciences* Vol. 42(1), pp. 35-41, February 2013
- [31] Abd El Wahab M. and El Nahas H.A. (2012). Radionuclides measurements and mineralogical studies on beach sands, East Rosetta Estuary, Egypt. *Chin. J. Geochem.* (2013)32:146–156. DOI:10.1007/s11631-013-0617-3
- [32] H.S Eissa, M.E. Medhat, S.A Said, and E.K. Elmaghraby (2010). Radiation dose estimation of sand samples collected from different Egyptian beaches. *Radiation Protection Dosimetry*, Vol. 147, No. 4, pp. 533–540.
- [33] N. Harikrishnan et al. (2017). An Evaluation of Natural Radioactivity and Its Associated Health Hazards Indices of Coastal Sediments from Rameshwaram Island, Tamilnadu, India. *Journal of Radiation and Nuclear Applications* 2, No. 1, 23-27
- [34] Derin MT, Vijayagopal P, Venkatraman B, Chaubey RC, Gopinathan A. (2012). Radionuclides and Radiation Indices of High Background Radiation Area in Chavara-Neendakara Placer Deposits (Kerala, India). *PLoS ONE* 7(11):e50468. doi:10.1371/journal.pone.0050468
- [35] V. Ramasamy, I.S. Senthil, V. Meenakshisundaram and V. Gajendran. (2009). Measurement of Natural Radioactivity In Beach Sediments From North East Coast of Tamilnadu, India. *Research Journal of Applied Sciences, Engineering and Technology* 1(2): 54-58
- [36] P. Mahawatte and K.N.R. Fernando. (2013). Radioactivity levels in beach sand from the West Coast of Sri Lanka. *Journal of the National Science Foundation of Sri Lanka* 41(4): 279-285
- [37] Z. Korkulu and N. Özkan (2008). Determination of natural radioactivity levels of beach sand samples in the black sea coast of Kocaeli (Turkey). *Radiation Physics and Chemistry*, Volume 88, Pages 27-31
- [38] S. Aközcan, (2012). Distribution of natural radionuclide concentrations in sediment samples in Didim and Izmir Bay (Aegean Sea-Turkey). *Journal of Environmental Radioactivity*, Volume 112, Pages 60-63
- [39] M.R. Zare, M. Mostajaboddavati, M. Kamali, M.R. Abdi, Mortazavi, M.Sc. (2012). <sup>235</sup>U, <sup>238</sup>U, <sup>232</sup>Th, <sup>40</sup>K and <sup>137</sup>Cs activity concentrations in marine sediments along the northern coast of Oman Sea using high-resolution gamma-ray spectrometry. *Marine Pollution Bulletin*, Volume 64, Pages 1956-1961, Issue 9, September 2012
- [40] A.A. El-Kammar, A.A. Ragab and M.I. Moustafa. (2010). Geochemistry of Economic Heavy Minerals from Rosetta Black Sand of Egypt. *JAKU: Earth Sci.*, Vol. 22, No. 2, pp: 69-97 (2011 A.D. / 1432 A.H.) DOI: 10.4197 / Ear. 22-2.4.